IEEE Access
Multidisciplinary | Rapid Review | Open Access Journal

SPECIAL SECTION ON ENERGY HARVESTING TECHNOLOGIES FOR WEARABLE AND IMPLANTABLE DEVICES

Received September 28, 2020, accepted October 14, 2020, date of publication October 19, 2020, date of current version October 30, 2020.

Digital Object Identifier 10.1109/ACCESS.2020.3032120

Transceiver Design for SWIPT MIMO Relay Systems With Hybridized Power-Time Splitting-Based Relaying Protocol

JUSTIN LEE BING[1], (Student Member, IEEE), YUE RONG[2], (Senior Member, IEEE), LENIN GOPAL[1], (Member, IEEE), AND CHOO W. R. CHIONG[1], (Member, IEEE)

[1]Department of Electrical and Computer Engineering, Curtin University Malaysia, Miri 98009, Malaysia
[2]School of Electrical Engineering, Computing and Mathematical Sciences, Curtin University, Perth, WA 6102, Australia

Corresponding author: Yue Rong (y.rong@curtin.edu.au)

ABSTRACT In this paper, we investigate a dual-hop simultaneous wireless information and power transfer (SWIPT) based amplifying-and-forward (AF) multiple-input multiple-output (MIMO) relay communication system where the relay node harvests energy based on radio frequency (RF) signals transmitted from the source node through the hybridized power-time splitting-based relaying (HPTSR) protocol to forward information to the destination node. The joint optimization of the time-switching (TS) factor, source and relay precoding matrices, and the power-splitting (PS) ratio vector is proposed to maximize the mutual information (MI) between the source and destination nodes. We derive the optimal structure for the source and relay precoding matrices to simplify the transceiver optimization problem. Two algorithms based on the upper bound and lower bound of the objective function are proposed to efficiently solve the optimization problem with low computational complexity. Numerical examples demonstrate that the proposed algorithms provide a better MI performance compared with TS based and PS based energy harvesting (EH) relay systems.

INDEX TERMS Amplify-and-forward (AF) relay, energy harvesting, hybridized power-time switching relaying (HPTSR), multiple-input multiple-output (MIMO) relay, simultaneous wireless information and power transfer (SWIPT).

I. INTRODUCTION

The number of wireless devices around the world is having a skyrocketing increase for the past few years. However, the performance of these devices is highly limited due to their finite lifetime and tight energy constraint. Even though battery replacing is a solution to prolong the lifetime of those devices, physical and/or economic constraints often make it hard to perform battery replacing for the devices. For instance, some wireless devices are lodged inside building structures or human bodies to collect information [1]. Thus, energy harvesting (EH) is suggested as an alternative solution that can prolong the lifetime of wireless devices [2]. Conventional EH methods have limitations as they heavily rely on natural resources to harvest energy which is unreliable as natural resources are difficult to manage. Thus conventional EH methods are not convenient to provide reliable energy sources to wireless devices. To overcome the limitation of conventional EH methods, a new EH method that can harvest energy from radio frequency (RF) signals is proposed to provide stable and controllable wireless energy supply [3]. Moreover, the EH method based on RF signals has noticeable advantages for wireless networks as RF signals are not only used for transferring power but also for delivering information. The EH method which exploits the usage of RF signals in wireless power transfer (WPT) and wireless information transfer (WIT) simultaneously is known as simultaneous wireless information and power transfer (SWIPT) [4].

In [5], an ideal SWIPT receiver design is proposed to perform information decoding (ID) and EH simultaneously, and the trade-off between the harvested energy and achievable mutual information (MI) rate is investigated using the capacity-energy function. However, the ideal SWIPT receiver has limitations in practical applications [6] as EH-circuits in practice are unable to perform ID for the information carried in the same signals directly. Two SWIPT receiver architectures, namely the time-switching (TS) protocol and the power-splitting (PS) protocol, are presented in [6] to overcome the limitation through coordinated WIT and WPT at the receiver.

The associate editor coordinating the review of this manuscript and approving it for publication was Abdul Halim Miah.

This work is licensed under a Creative Commons Attribution 4.0 License. For more information, see https://creativecommons.org/licenses/by/4.0/

The PS and TS protocols for the SWIPT receiver are extended in [7] to relay communication systems by introducing TS-based and PS-based relaying protocols to perform EH and ID at the relay node. Relay technology is commonly used to extend the network coverage of wireless communication [8]. A relay node implemented in a SWIPT relay communication system with the EH relaying protocol introduced in [7] is capable of performing EH and ID from the received signals transmitted from the source node. The SWIPT relay node exploits the harvested energy to process and forward the received signals to the destination node. Relay communication systems with SWIPT relay nodes have been investigated in [9]–[14]. In [9], a cooperative communication system is investigated where multiple pairs of transmitter-receiver interact with each other through an EH relay node where the focus is on the relay's strategies regarding user power allocation of the harvested energy and influences on the system performance. In [10], the authors designed a game-theoretical scheme to tackle the power distribution problem for SWIPT in interference relay communication networks. In [11], the harvest-use and harvest-use-store models are investigated with full duplex EH relay communication systems using the PS-based relaying protocol. In [12], the impact of co-channel interference (CCI) towards a wireless communication system using a SWIPT full duplex relay with the PS-based relaying protocol has been studied. In [13], the achievable rate of full duplex relay communication systems is studied on both the amplify-and-forward (AF) relaying scheme as well as the decode-and-forward (DF) relaying scheme under the TS-based EH relay protocol. In [14], the authors investigated the influence of decoding cost towards the performance of the communication system with a DF relay using the PS-based protocol while the decoding cost is introduced at both the relay and destination nodes to perform ID by deriving and optimizing the system achievable rate.

By installing multiple antennas at nodes in wireless communication systems, the multiple-input multiple-output (MIMO) technique is famous for its capability in boosting the spectral and energy efficiency of communication systems [15]. With multiple antennas at nodes compared with single-antenna, RF energy transmission to wireless devices is more efficient. Studies regarding the application of SWIPT in MIMO relay communication systems have emerged rapidly in recent years [1], [16]–[25]. In [1], an AF MIMO orthogonal frequency-division multiplexing (OFDM) EH relay communication system adopted with TS-based and PS-based EH relaying protocols is investigated by jointly optimizing multiple system configuration parameters to achieve the maximum achievable rate. In [16], the rate-stored energy (R-E) region which demonstrates the energy-rate tradeoffs under several EH relaying schemes in a SWIPT MIMO relay communication system is investigated. Moreover, the challenges faced in this research field are introduced and discussed in [16]. In [17], the performance tradeoff of an orthogonal space-time block-code (OSTBC)-based non-regenerative MIMO OFDM relay communication system with two destination nodes performing EH and ID separately is investigated where the joint source and relay precoder optimization problem is proposed to achieve the R-E region which characterizes the system performance tradeoff. In [18], the authors investigated the relay matrix optimization of a communication system with single-antenna source and destination nodes and a multi-antenna relay node. In [19], two approaches which are known as the iterative algorithm and the channel diagonalization-based algorithm are developed to solve the joint source and relay precoder optimization problem in wireless powered MIMO relay networks. In [20], a SWIPT MIMO relay communication system with PS-based relaying scheme is investigated with iterative algorithms for uniform and arbitrary source precoding scenarios. In [21], the joint optimization problem of a source precoding matrix, relay matrix, and PS factor matrix is solved with the sequential quadratic programming (SQP) approach, the semi-definite programming (SDP) approach and the primal-dual search approach. The optimization problem for SWIPT MIMO relay communication systems with TS-based relaying scheme is investigated in [22] for non-regenerative relays. In [23], the works of [21] and [22] are extended to regenerative relaying scheme. In [24], a SWIPT MIMO AF relay communication system is investigated by designing the optimal source matrix and relay matrix to characterize the R-E region defined by the achievable rate of the system and harvested energy at the relay node for the ideal EH scheme, the PS relaying scheme, and the TS relaying scheme. In [25], the work of [24] is extended to the DF relaying scheme with possibly imperfect channel knowledge.

A dual-hop MIMO relay communication system with an EH relay node using the AF relaying protocol is investigated in this paper. Relay nodes play an important role in communication systems where the direct link between the source and destination node is unavailable due to shadowing and pathloss effects [1], [17], [20]–[25]. Different from existing works using the PS-based EH relaying protocol [1], [20], [21], [24], [25] and the TS-based EH relaying protocol [1], [22]–[25], to increase the energy harvested at the relay node, which is expected to provide a better performance of the proposed system, a hybrid EH scheme which is known as hybridized power-time splitting-based relaying (HPTSR) protocol is adopted at the relay node. The HPTSR scheme works by transmitting energy-bearing RF signals to the relay node for EH in the first time slot while transmitting information-carrying RF signals to the relay node for ID in the second time slot, In particular, in the second time slot, the received signals are split into two portions for EH and ID, respectively. Therefore, this paper extends existing EH relaying protocols to the HPTSR protocol. Introducing PS in the second time slot provides additional degrees of freedom to optimize the system performance. For instance, if the relay node requires additional power, instead of adjusting a single TS factor to allow additional time for energy harvesting as in the TS protocol, which affects *all sub-channels*, introducing

PS in the second time slot allows adjusting the PS ratio in *each sub-channel* for an optimal energy harvesting and information transmission.

It is noted that several existing works have considered the HPTSR protocol [26]–[29]. However, the system nodes in previous research are installed with one antenna and as mentioned before, MIMO techniques provide a better performance for SWIPT communication systems. Our paper extends the HPTSR protocol from single-input single-output (SISO) relay communication systems to MIMO relay communication systems. Moreover, compared with existing PS-based MIMO relay systems where a constant PS ratio is usually adopted for all antennas [18]–[20], [24], [25], a more general system with corresponding PS ratio for each antenna is considered in this paper, which enhances the system performance.

We would like to mention that the transceiver optimization problem is much more challenging in a HPTSR-based MIMO relay system. To solve this problem, we first derive the optimal structure of the source and relay precoding matrices, which simplifies the transceiver optimization problem to a low complexity power allocation problem with scalar variables. However, this power allocation problem is still non-convex. To tackle this problem, we develop two approaches by exploiting the upper and lower bounds of the objective function, respectively. We show that both the upper bound and lower bound based problems can be converted to convex optimization problems, which can be solved with low computational complexity. Simulation results show that the proposed HPTSR based MIMO relay system achieves better performance compared with existing approaches.

The rest of this paper is organized as follows. In Section II, the model of a dual-hop AF SWIPT MIMO relay system with the HPTSR protocol is introduced. In Section III, we formulate the optimization problem for the proposed transceiver design and simplify it to a power allocation problem by adopting the proposed optimal structure for precoding matrices. To solve the power allocation problem, a lower bound based algorithm is derived in Section IV and an upper bound based algorithm is developed in Section V. In Section VI, numerical examples are displayed to illustrate the performance of the proposed algorithm compared with existing works. In Section VII, the paper is concluded.

II. SYSTEM MODEL

Let us consider a dual-hop three-node MIMO relay communication system where the source node transmits information signals to the destination node with the help of a single relay node as displayed in Fig. 1. The source, relay, and destination nodes are installed with N_s, N_r, and N_d antennas, respectively. We assume the source node is equipped with its power supply. Besides, the relay node requires to be powered by energy harvested from received RF signals. In a single communication cycle, there are two phases. The source node transmits energy-carrying and information-bearing signals to the relay node in the source phase. The energy-carrying signals are

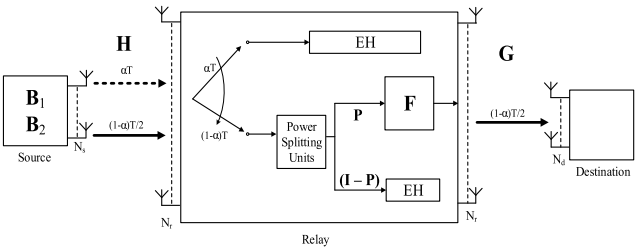

FIGURE 1. Block diagram of a dual-hop AF SWIPT MIMO relay system with the HPTSR protocol.

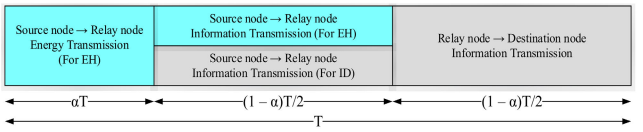

FIGURE 2. The diagram of the HPTSR protocol.

harvested by the relay node with the TS protocol, while the information-bearing signals are directed to the PS unit to undergo EH and ID with the PS protocol. Due to the simplicity of the AF relaying scheme, it is implemented at the relay node. Moreover, the AF scheme reduces the decoding cost required in a DF scheme for decoding and re-encoding the received signals which helps in energy saving. Thus, with the AF scheme, the portion of information-bearing signals at the relay node for ID is linearly precoded and transmitted to the destination node at the relay phase. We assume the direct-link between the source and destination nodes does not exist due to severe pathloss and shadowing. We also assume that the synchronization between the source, relay, and destination nodes is perfect.

The diagram of the HPTSR protocol is shown in Fig. 2. It can be seen that the total time of one communication cycle T is divided into three time-intervals. In the first time-interval, for a duration of αT, the energy-carrying signal is transferred from the source node to the relay node, where $\alpha \in [0, 1]$ represents the TS factor. In the second time-interval, for a duration of $(1-\alpha)T/2$, the source node transmits the information-bearing signal to the relay node. Then, the received signal at the ith antenna of the relay node is split into two independent signal streams with a PS ratio of p_i, where $p_i \in [0, 1]$ for $i = 1, \cdots, N_r$. One of the signal streams with a power ratio of p_i is sent towards the ID receiver while the other signal stream with a power ratio of $(1 - p_i)$ is sent towards the EH receiver. In the last time-interval, for the remaining duration of $(1-\alpha)T/2$, the relay node precodes the signal stream at the ID receiver and transmits the precoded signal to the destination node. We assume $T = 1$ in this paper for simplicity purposes.

During the first time-interval, the energy-carrying signal vector $\mathbf{s}_1 \in \mathbb{C}^{N_1 \times 1}$ with a covariance matrix given by $E\{\mathbf{s}_1\mathbf{s}_1^H\} = \mathbf{I}_{N_1}$ is transmitted from the source node with the source precoding matrix $\mathbf{B}_1 \in \mathbb{C}^{N_s \times N_1}$ to the relay node, where $\mathbf{I}_n$ is an identity matrix of size $n \times n$, $E\{\cdot\}$ denotes the statistical expectation, and $(\cdot)^H$ stands for the Hermitian transpose. Thus, the received signal at the first time-interval

$\mathbf{y}_{r,1}$ at the relay node is given as

$$\mathbf{y}_{r,1} = \mathbf{H}\mathbf{B}_1\mathbf{s}_1 + \mathbf{n}_{r,1} \tag{1}$$

where $\mathbf{H} \in \mathbb{C}^{N_r \times N_s}$ is the MIMO channel matrix between the source and relay nodes, while $\mathbf{n}_{r,1} \in \mathbb{C}^{N_r \times 1}$ is the additive white Gaussian noise (AWGN) vector at the relay node during the first time-interval. From (1), the RF energy harvested during the first time-interval at the relay node without the noise component [30] is written as

$$E_{r,1} = \alpha\eta \; tr\{\mathbf{H}\mathbf{B}_1\mathbf{B}_1^H\mathbf{H}^H\} \tag{2}$$

where $\eta \in [0, 1]$ is the conversion efficiency at the relay node and $tr\{\cdot\}$ denotes the matrix trace.[1]

During the second time-interval, the information-bearing signal vector $\mathbf{s}_2 \in \mathbb{C}^{N_2 \times 1}$ with a covariance matrix given as $E\{\mathbf{s}_2\mathbf{s}_2^H\} = \mathbf{I}_{N_2}$ is transmitted from the source node with the source precoding matrix $\mathbf{B}_2 \in \mathbb{C}^{N_s \times N_2}$ to the relay node. The received signal at second time-interval $\mathbf{y}_{r,2}$ at the relay node is given as

$$\mathbf{y}_{r,2} = \mathbf{H}\mathbf{B}_2\mathbf{s}_2 + \mathbf{n}_{r,2} \tag{3}$$

where $\mathbf{n}_{r,2} \in \mathbb{C}^{N_r \times 1}$ with a covariance matrix of $E\{\mathbf{n}_{r,2}\mathbf{n}_{r,2}^H\} = \sigma_r^2\mathbf{I}_{N_r}$ is the AWGN vector at the relay node during the second time-interval. At the relay node, the received signal (3) is split into two signal vectors with a diagonal PS matrix $\mathbf{P} = \text{diag}(p_1, \cdots, p_{N_r})$, where $\mathbf{P}^{\frac{1}{2}}\mathbf{y}_{r,2}$ is for information transmission and $(\mathbf{I}_{N_r} - \mathbf{P})^{\frac{1}{2}}\mathbf{y}_{r,2}$ is for energy harvesting. Here diag$(\cdot)$ denotes a diagonal matrix. The RF energy harvested during the second time-interval at the relay node without the noise component [30] is written as

$$E_{r,2} = \frac{1-\alpha}{2}\eta \; tr\{(\mathbf{I}_{N_r} - \mathbf{P})\mathbf{H}\mathbf{B}_2\mathbf{B}_2^H\mathbf{H}^H\}. \tag{4}$$

From (2) and (4), the total available transmission energy at the relay node obtained from the RF energy harvested during the first and second time intervals is given as

$$E_r = \alpha\eta \; tr\{\mathbf{H}\mathbf{B}_1\mathbf{B}_1^H\mathbf{H}^H\} + \frac{1-\alpha}{2}\eta \; tr\{(\mathbf{I}_{N_r} - \mathbf{P})\mathbf{H}\mathbf{B}_2\mathbf{B}_2^H\mathbf{H}^H\}. \tag{5}$$

During the last time-interval, the linearly precoded signal vector $\mathbf{x}_r$ given by

$$\mathbf{x}_r = \mathbf{F}\mathbf{P}^{\frac{1}{2}}\mathbf{y}_{r,2} \tag{6}$$

is transmitted to the destination node, where $\mathbf{F} \in \mathbb{C}^{N_r \times N_r}$ is the relay precoding matrix. The received signal at the destination node is given as

$$\begin{aligned}\mathbf{y}_d &= \mathbf{G}\mathbf{x}_r + \mathbf{n}_d \\ &= \mathbf{G}\mathbf{F}\mathbf{P}^{\frac{1}{2}}\mathbf{H}\mathbf{B}_2\mathbf{s}_2 + \mathbf{G}\mathbf{F}\mathbf{n}_{r,2} + \mathbf{n}_d\end{aligned} \tag{7}$$

where $\mathbf{G} \in \mathbb{C}^{N_d \times N_r}$ is the MIMO channel matrix between the relay and destination nodes and $\mathbf{n}_d \in \mathbb{C}^{N_d \times 1}$ is the AWGN vector at the destination node with a covariance matrix of $E\{\mathbf{n}_d\mathbf{n}_d^H\} = \sigma_d^2\mathbf{I}_{N_d}$. From (7), the mutual information between source and destination is written as

$$\text{MI}(\alpha, \mathbf{P}, \mathbf{B}_2, \mathbf{F}) = \frac{1-\alpha}{2} \log\Big|\mathbf{I}_{N_2} + \mathbf{B}_2^H\mathbf{H}^H\mathbf{P}^{\frac{1}{2}}\mathbf{F}^H\mathbf{G}^H \big(\sigma_r^2\mathbf{G}\mathbf{F}\mathbf{F}^H\mathbf{G}^H + \sigma_d^2\mathbf{I}_{N_d}\big)^{-1}\mathbf{G}\mathbf{F}\mathbf{P}^{\frac{1}{2}}\mathbf{H}\mathbf{B}_2\Big| \tag{8}$$

where $(\cdot)^{-1}$ denotes the matrix inverse and $|\cdot|$ stands for the matrix determinant. We assume the MIMO channel matrices $\mathbf{H}$ and $\mathbf{G}$ are fully-known by the relay and destination nodes, respectively. Moreover, the value of N_2 is set to satisfy $N_2 < \min(\text{rank}(\mathbf{H}), \text{rank}(\mathbf{G}))$ and $\text{rank}(\mathbf{B}_2) = \text{rank}(\mathbf{F}) = N_2$ in order not to waste the transmission power available at the source and relay nodes.

The required transmission energy at the source node to transmit signal vectors $\mathbf{s}_1$ and $\mathbf{s}_2$ is written as the following, respectively

$$E_{u,s,1} = \alpha \; tr\{\mathbf{B}_1\mathbf{B}_1^H\} \tag{9}$$

$$E_{u,s,2} = \frac{1-\alpha}{2} \; tr\{\mathbf{B}_2\mathbf{B}_2^H\} \tag{10}$$

where the total transmission energy required by the source node can be consider as $E_{u,s} = E_{u,s,1} + E_{u,s,2}$. Thus, the transmission energy constraint at the source node is considered as

$$E_{u,s} \le \frac{1+\alpha}{2}P_s \tag{11}$$

where $P_s > 0$ is the power budget available at the source node. In [1], the authors assumed that a constant power is used for both energy-transferring and information-bearing signal transmission which is given by

$$tr\{\mathbf{B}_1\mathbf{B}_1^H\} \le P_s \quad tr\{\mathbf{B}_2\mathbf{B}_2^H\} \le P_s. \tag{12}$$

It is noticeable that (12) is a special example of (11). In other words, (11) has a larger feasible region compared to (12). It can be observed the source precoding matrices $\mathbf{B}_1$ and $\mathbf{B}_2$ are connected through a single energy constraint in (11). This enables the source node to transmit at different power levels accommodated to the purpose of energy-transferring and information transmission. Thus, (11) is more general than (12) and the transceiver designs proposed under (11) are expected to provide a better performance compared to the transceiver designs proposed under (12).

From (6), the transmission energy required by the relay node is written as

$$E_{u,r} = \frac{1-\alpha}{2} \; tr\{\mathbf{F}(\mathbf{P}^{\frac{1}{2}}\mathbf{H}\mathbf{B}_2\mathbf{B}_2^H\mathbf{H}^H\mathbf{P}^{\frac{1}{2}} + \sigma_r^2\mathbf{I}_{N_r})\mathbf{F}^H\}. \tag{13}$$

All energy harvested at the relay node given by (5) is used to transmit information signals received from the source node to the destination node. Thus, the transmission energy constraint for the relay node is considered as

$$E_{u,r} \le E_r. \tag{14}$$

The objective in the proposed transceiver design is to maximize the mutual information (8) between the source and destination nodes subjecting to energy constraints at the source

[1] It is shown [31]–[34] that in practice the energy harvesting efficiency is a function of input power, and for input power below the harvesting circuit power sensitivity threshold, the harvested power can be zero. In this paper, similar to [1], [22], [35], we assume a simplified linear energy harvesting model with a constant η. Note that the algorithms proposed in this paper can be applied to any given η.

and the relay nodes given by (11) and (14), respectively. From (8), (11), and (14), the transceiver optimization problem for dual-hop HPTSR-based AF MIMO relay systems can be written as

$$\max_{\alpha,\mathbf{P},\mathbf{B}_1,\mathbf{B}_2,\mathbf{F}} \quad \mathrm{MI}(\alpha,\mathbf{P},\mathbf{B}_2,\mathbf{F}) \tag{15a}$$

$$s.t.\ \alpha tr\{\mathbf{B}_1\mathbf{B}_1^H\}+\frac{1-\alpha}{2}tr\{\mathbf{B}_2\mathbf{B}_2^H\}\le\frac{1+\alpha}{2}P_s \tag{15b}$$

$$\frac{1-\alpha}{2}tr\{\mathbf{F}(\mathbf{P}^{\frac{1}{2}}\mathbf{H}\mathbf{B}_2\mathbf{B}_2^H\mathbf{H}^H\mathbf{P}^{\frac{1}{2}}+\sigma_r^2\mathbf{I}_{N_r})\mathbf{F}^H\}$$
$$\le\alpha\eta\ tr\{\mathbf{H}\mathbf{B}_1\mathbf{B}_1^H\mathbf{H}^H\}+$$
$$\frac{1-\alpha}{2}\eta\ tr\{(\mathbf{I}_{N_r}-\mathbf{P})\mathbf{H}\mathbf{B}_2\mathbf{B}_2^H\mathbf{H}^H\} \tag{15c}$$

$$0\le p_i\le 1,\quad i=1,\cdots,N_r \tag{15d}$$

$$0\le\alpha\le 1. \tag{15e}$$

III. PROPOSED TRANSCEIVER DESIGN

It is noticeable that the problem (15a) is nonconvex in nature with matrix variables which is quite hard to solve. Moreover, compared with existing TS and PS based system designs, the transmission energy constraint (15c) from the HPTSR protocol further increases the technical difficulty in solving the problem (15a). In this section, we derive the optimal structure of $\mathbf{B}_1$, $\mathbf{B}_2$, and $\mathbf{F}$ to solve the nonconvex optimization problem (15a).

It can be observed that $\mathbf{B}_1$ is not in the objective function (15a), but it can influence (15a) by varying the feasible region of the problem (15a) specified by constraints (15b) and (15c). Thus, in order to maximize the feasible region of the problem (15a), for any $tr\{\mathbf{B}_1\mathbf{B}_1^H\}$ in the left-hand side of (15b), it is important to maximize $tr\{\mathbf{H}\mathbf{B}_1\mathbf{B}_1^H\mathbf{H}^H\}$ in the right-hand side of (15c). This constrained maximization problem can be formulated as the problem below [1], [22]

$$\max_{\mathbf{B}_1} tr\{\mathbf{H}\mathbf{B}_1\mathbf{B}_1^H\mathbf{H}^H\} \tag{16a}$$

$$s.t.\ tr\{\mathbf{B}_1\mathbf{B}_1^H\}=\lambda_1 \tag{16b}$$

where λ_1 is a positive scalar value. Let us introduce $\mathbf{H}=\mathbf{U}_h\mathbf{\Lambda}_h^{\frac{1}{2}}\mathbf{V}_h^H$ as the singular value decomposition (SVD) of $\mathbf{H}$ with the diagonal elements of $\mathbf{\Lambda}_h$ arranged in descending order. Let us also introduce the eigenvalue decomposition (EVD) of $\mathbf{B}_1\mathbf{B}_1^H$ as $\mathbf{U}_b\mathbf{\Lambda}_b\mathbf{U}_b^H$, where the diagonal elements of $\mathbf{\Lambda}_b$ are arranged in descending order, too. Based on [36], the following inequality is given as

$$tr\{\mathbf{U}\mathbf{V}\}=\sum_i\lambda_i(\mathbf{U}\mathbf{V})\le\sum_i\lambda_i(\mathbf{U})\lambda_i(\mathbf{V}) \tag{17}$$

where $\lambda_i(\mathbf{X})$ indicates the ith eigenvalue of $\mathbf{X}$ and $\lambda_i(\mathbf{U})$ and $\lambda_i(\mathbf{V})$ are arranged in the same order. By applying (17), the SVD of $\mathbf{H}$, and the EVD of $\mathbf{B}_1\mathbf{B}_1^H$, (16a) can be upper-bounded by

$$tr\{\mathbf{H}\mathbf{B}_1\mathbf{B}_1^H\mathbf{H}^H\}=tr\{\mathbf{\Lambda}_h\mathbf{\Lambda}_b\}\le\sum_{i=1}^{N_s}\lambda_{h,i}\lambda_{b,i} \tag{18}$$

where $\lambda_{h,i}$ and $\lambda_{b,i}$ are the ith diagonal entry of $\mathbf{\Lambda}_h$ and $\mathbf{\Lambda}_b$, respectively. It is noticeable in (18) that the equality is achieved when $\mathbf{U}_b=\mathbf{V}_h\tilde{\mathbf{I}}$, where $\tilde{\mathbf{I}}\in\mathbb{C}^{N_s\times N_s}$ is a diagonal matrix with unit norm diagonal elements. For simplicity, $\tilde{\mathbf{I}}$ is set to be $\mathbf{I}_{N_s}$ and $\mathbf{U}_b=\mathbf{V}_h$. Thus, by exploiting the upper bound in (18), the optimization problem (16a) is rewritten into

$$\max_{\{\lambda_{b,i}\}}\ \sum_{i=1}^{N_s}\lambda_{h,i}\lambda_{b,i} \tag{19a}$$

$$s.t.\ \sum_{i=1}^{N_s}\lambda_{b,i}=\lambda_1 \tag{19b}$$

where $\{\lambda_{b,i}\}=\{\lambda_{b,i},i=1,\cdots,N_s\}$. The solution to the problem (19a) is $\lambda_{b,1}=\lambda_1$ which results in $\mathbf{B}_1\mathbf{B}_1^H=\lambda_1\mathbf{v}_{h,1}\mathbf{v}_{h,1}^H$ where $\mathbf{v}_{h,1}$ is the first column of $\mathbf{V}_h$. Therefore, the optimal structure for $\mathbf{B}_1$ is given by

$$\mathbf{B}_1=\lambda_1^{\frac{1}{2}}\mathbf{v}_{h,1}\mathbf{v}^H \tag{20}$$

where $\mathbf{v}$ can be any $N_1\times 1$ vector with $\mathbf{v}^H\mathbf{v}=1$. It is interesting to note that the optimal $\mathbf{B}_1$ derived in (20) has a rank-1 structure matched to $\mathbf{v}_{h,1}$. Thus, to maximize the energy harvested at the relay node, all transmission power during the first time interval at the source node is allocated to the channel linked to the largest singular value of $\mathbf{H}$. In other words, only λ_1 need to be optimized in $\mathbf{B}_1$ and $tr\{\mathbf{B}_1\mathbf{B}_1^H\}=\lambda_1$. By applying (20), the optimization problem (15) is equivalently converted to

$$\max_{\alpha,\lambda_1,\mathbf{P},\mathbf{B}_2,\mathbf{F}}\ \frac{1-\alpha}{2}\log\Big|\mathbf{I}_{N_2}+\mathbf{B}_2^H\mathbf{H}^H\mathbf{P}^{\frac{1}{2}}\mathbf{F}^H\mathbf{G}^H\big(\sigma_r^2\mathbf{G}\mathbf{F}\mathbf{F}^H\mathbf{G}^H+\sigma_d^2\mathbf{I}_{N_d}\big)^{-1}\mathbf{G}\mathbf{F}\mathbf{P}^{\frac{1}{2}}\mathbf{H}\mathbf{B}_2\Big| \tag{21a}$$

$$s.t.\ \alpha\lambda_1+\frac{1-\alpha}{2}tr\{\mathbf{B}_2\mathbf{B}_2^H\}\le\frac{1+\alpha}{2}P_s \tag{21b}$$

$$tr\{\mathbf{F}(\mathbf{P}^{\frac{1}{2}}\mathbf{H}\mathbf{B}_2\mathbf{B}_2^H\mathbf{H}^H\mathbf{P}^{\frac{1}{2}}+\sigma_r^2\mathbf{I}_{N_r})\mathbf{F}^H\}\le$$
$$\kappa\eta\lambda_1+\eta\ tr\{(\mathbf{I}_{N_r}-\mathbf{P})\mathbf{H}\mathbf{B}_2\mathbf{B}_2^H\mathbf{H}^H\} \tag{21c}$$

$$0\le p_i\le 1,\quad i=1,\cdots,N_r \tag{21d}$$

$$0\le\alpha\le 1 \tag{21e}$$

where $\kappa=2\alpha\lambda_{h,1}/(1-\alpha)$.

By applying the Weinstein-Aronszajn identity [37], the objective function (21a) can be rewritten as

$$\frac{1-\alpha}{2}\log\Big|\mathbf{I}_{N_d}+\mathbf{G}\mathbf{F}\mathbf{\Xi}\mathbf{F}^H\mathbf{G}^H\big(\sigma_r^2\mathbf{G}\mathbf{F}\mathbf{F}^H\mathbf{G}^H+\sigma_d^2\mathbf{I}_{N_d}\big)^{-1}\Big| \tag{22}$$

where $\mathbf{\Xi}=\mathbf{P}^{\frac{1}{2}}\mathbf{H}\mathbf{B}_2\mathbf{B}_2^H\mathbf{H}^H\mathbf{P}^{\frac{1}{2}}$ is considered and designed into a diagonal matrix as based on the Hadamard's inequality [38] on matrix determinant, the objective function (22) is maximized when $\mathbf{G}\mathbf{F}\mathbf{\Xi}\mathbf{F}^H\mathbf{G}^H\big(\sigma_r^2\mathbf{G}\mathbf{F}\mathbf{F}^H\mathbf{G}^H+\sigma_d^2\mathbf{I}_{N_d}\big)^{-1}$ is diagonal. For any given value of α, λ_1, P, and $\mathbf{B}_2$, the optimization problem for $\mathbf{F}$ is viewed as

$$\max_{\mathbf{F}}\ \frac{1-\alpha}{2}\log\Big|\mathbf{I}_{N_d}+\mathbf{G}\mathbf{F}\mathbf{\Xi}\mathbf{F}^H\mathbf{G}^H\big(\sigma_r^2\mathbf{G}\mathbf{F}\mathbf{F}^H\mathbf{G}^H+\sigma_d^2\mathbf{I}_{N_d}\big)^{-1}\Big| \tag{23a}$$

$$s.t.\ tr\{\mathbf{F}(\mathbf{\Xi}+\sigma_r^2\mathbf{I}_{N_r})\mathbf{F}^H\}\le$$
$$\kappa\eta\lambda_1+\eta\ tr\{(\mathbf{I}_{N_r}-\mathbf{P})\mathbf{H}\mathbf{B}_2\mathbf{B}_2^H\mathbf{H}^H\}. \tag{23b}$$

Let us introduce the SVD of $\mathbf{G}$ as $\mathbf{G} = \mathbf{U}_g \mathbf{\Lambda}_g^{\frac{1}{2}} \mathbf{V}_g^H$ with the diagonal elements of $\mathbf{\Lambda}_g$ sorted in descending order. From [39], it is noted that the optimal structure of $\mathbf{F}$ under the optimization problem (23a) with a diagonal $\mathbf{\Xi}$ is given as

$$\mathbf{F} = \mathbf{V}_g \dot{\mathbf{\Lambda}}_f^{\frac{1}{2}} \tag{24}$$

where $\dot{\mathbf{\Lambda}}_f \in \mathbb{C}^{N_r \times N_r}$ is a diagonal matrix. As the maximal number of concurrent data streams for information transmission by the relay system is N_2, the optimal $\dot{\mathbf{\Lambda}}_f = \text{bd}(\mathbf{\Lambda}_f, \mathbf{0}_{N_r - N_2})$ where $\mathbf{\Lambda}_f \in \mathbb{C}^{N_2 \times N_2}$ is a diagonal matrix, and $\mathbf{0}_m$ is a zero matrix of size $m \times m$ and $\text{bd}(\cdot)$ represents a block diagonal matrix. Similarly, with the consideration of the maximal number of concurrent data streams, the optimal $\mathbf{P}$ is given as $\text{bd}(\mathbf{P}_M, \mathbf{0}_{N_r - N_2})$, where $\mathbf{P}_M \in \mathbb{C}^{N_2 \times N_2}$ is a diagonal matrix containing the PS ratios p_i for $i = 1, \cdots, N_2$. In other words, the remaining $N_r - N_2$ antennas are solely used for EH with the corresponding PS ratios set to 0.

We introduce the following to design $\mathbf{\Xi}$ into a diagonal matrix for maximizing the objective function (22)

$$\mathbf{H}_M \mathbf{B}_2 \mathbf{B}_2^H \mathbf{H}_M^H = \mathbf{\Lambda}_2 \tag{25}$$

where $\mathbf{H}_M$ contains the first N_2 rows of $\mathbf{H}$ and $\mathbf{\Lambda}_2 \in \mathbb{C}^{N_2 \times N_2}$ is a diagonal matrix. By introducing the SVD of $\mathbf{H}_M$ as $\mathbf{H}_M = \mathbf{U}_{h,1} \mathbf{\Lambda}_{h,1}^{\frac{1}{2}} \mathbf{V}_{h,1}^H$ where the diagonal entries of $\mathbf{\Lambda}_{h,1}$ are arranged in descending order, the optimal structure of $\mathbf{B}_2$ is proposed to be written as

$$\mathbf{B}_2 = \mathbf{V}_{h,1} \mathbf{\Lambda}_{h,1}^{-\frac{1}{2}} \mathbf{U}_{h,1}^H \mathbf{\Lambda}_2^{\frac{1}{2}}. \tag{26}$$

By applying the optimal structure of the precoding matrices $\mathbf{F}$ and $\mathbf{B}_2$ given by (24) and (26), respectively, the optimization problem (21a) is rewritten as

$$\max_{\alpha, \lambda_1, \mathbf{P}_M, \mathbf{\Lambda}_2, \mathbf{\Lambda}_f} \frac{1-\alpha}{2} \log \left| \mathbf{I}_{N_2} + \mathbf{\Lambda}_g \mathbf{\Lambda}_f \mathbf{P}_M \mathbf{\Lambda}_2 \left(\sigma_r^2 \mathbf{\Lambda}_g \mathbf{\Lambda}_f + \sigma_d^2 \mathbf{I}_{N_2} \right)^{-1} \right| \tag{27a}$$

$$s.t.\ \alpha \lambda_1 + \frac{1-\alpha}{2} tr\{\mathbf{\Lambda}_2 \mathbf{\Upsilon}\} \le \frac{1+\alpha}{2} P_s \tag{27b}$$

$$tr\{\mathbf{\Lambda}_f (\mathbf{P}_M \mathbf{\Lambda}_2 + \sigma_r^2 \mathbf{I}_{N_r})\} \le \kappa \eta \lambda_1 + \eta tr\left\{ (\mathbf{\Psi} - \mathbf{P}_M) \mathbf{\Lambda}_2 \right\} \tag{27c}$$

$$0 \le p_i \le 1, \quad i = 1, \cdots, N_2 \tag{27d}$$

$$0 \le \alpha \le 1 \tag{27e}$$

where $\mathbf{\Upsilon} = \mathbf{U}_{h,1} \mathbf{\Lambda}_{h,1}^{-1} \mathbf{U}_{h,1}^H$, $\mathbf{\Psi} = \mathbf{I}_{N_2} + \widehat{\mathbf{H}}^H \widehat{\mathbf{H}}$, $\widehat{\mathbf{H}} = \mathbf{H}_m \mathbf{V}_{h,1} \mathbf{\Lambda}_{h,1}^{-\frac{1}{2}} \mathbf{U}_{h,1}^H$, and $\mathbf{H}_m$ contains the last $N_r - N_2$ rows of $\mathbf{H}$. It is noticeable in (27a) that $\mathbf{\Lambda}_g$, $\mathbf{\Lambda}_f$, $\mathbf{P}_M$, and $\mathbf{\Lambda}_2$ are diagonal matrices, hence the problem (27) can be equivalently rewritten into the following power allocation problem with scalar variables

$$\max_{\alpha, \lambda_1, \mathbf{p}, \boldsymbol{\lambda}_2 \boldsymbol{\lambda}_f} \frac{1-\alpha}{2} \sum_{i=1}^{N_2} \log \left(1 + \frac{p_i \lambda_{2,i} \lambda_{f,i} \lambda_{g,i}}{\lambda_{f,i} \lambda_{g,i} + 1} \right) \tag{28a}$$

$$s.t.\ \alpha \lambda_1 + \frac{1-\alpha}{2} \sigma_r^2 \sum_{i=1}^{N_2} \delta_i \lambda_{2,i} \le \frac{1+\alpha}{2} P_s \tag{28b}$$

$$\sum_{i=1}^{N_2} \lambda_{f,i} (p_i \lambda_{2,i} + 1) \le \kappa \eta \lambda_1 + \eta \sigma_r^2 \sum_{i=1}^{N_2} (\varepsilon_i - p_i) \lambda_{2,i} \tag{28c}$$

$$\lambda_{2,i} \ge 0, \quad \lambda_{f,i} \ge 0 \tag{28d}$$

$$0 \le p_i \le 1, \quad i = 1, \cdots, N_2 \tag{28e}$$

$$0 \le \alpha \le 1 \tag{28f}$$

where $\lambda_{2,i} = \widetilde{\lambda}_{2,i} / \sigma_r^2$, $\lambda_{f,i} = \sigma_r^2 \widetilde{\lambda}_{f,i}$, $\lambda_{g,i} = \widetilde{\lambda}_{g,i} / \sigma_d^2$ for $i = 1, \cdots, N_2$, $\widetilde{\lambda}_{2,i}$, $\widetilde{\lambda}_{f,i}$, $\widetilde{\lambda}_{g,i}$, δ_i, and ε_i represent the ith diagonal elements of $\mathbf{\Lambda}_2$, $\mathbf{\Lambda}_f$, $\mathbf{\Lambda}_g$, $\mathbf{\Upsilon}$, and $\mathbf{\Psi}$ respectively, $\mathbf{p} = [p_1, \cdots, p_{N_2}]^T$, $\boldsymbol{\lambda}_2 = [\lambda_{2,1} \cdots, \lambda_{2,N_2}]^T$, $\boldsymbol{\lambda}_f = [\lambda_{f,1} \cdots, \lambda_{f,N_2}]^T$, and $(\cdot)^T$ denotes the matrix and vector transpose.

Let us introduce $z_i = \lambda_{f,i}(p_i \lambda_{2,i} + 1)$, $i = 1, \cdots, N_2$. Then the optimization problem (28) can be written as

$$\max_{\alpha, \lambda_1, \mathbf{p}, \mathbf{z}, \boldsymbol{\lambda}_2} \frac{1-\alpha}{2} \sum_{i=1}^{N_2} \log \left(1 + \frac{p_i z_i \lambda_{2,i} \lambda_{g,i}}{p_i \lambda_{2,i} + z_i \lambda_{g,i} + 1} \right) \tag{29a}$$

$$s.t.\ \alpha \lambda_1 + \frac{1-\alpha}{2} \sigma_r^2 \sum_{i=1}^{N_2} \delta_i \lambda_{2,i} \le \frac{1+\alpha}{2} P_s \tag{29b}$$

$$\sum_{i=1}^{N_2} z_i \le \kappa \eta \lambda_1 + \eta \sigma_r^2 \sum_{i=1}^{N_2} (\varepsilon_i - p_i) \lambda_{2,i} \tag{29c}$$

$$\lambda_{2,i} \ge 0, \quad z_i \ge 0 \tag{29d}$$

$$0 \le p_i \le 1, \quad i = 1, \cdots, N_2 \tag{29e}$$

$$0 \le \alpha \le 1 \tag{29f}$$

where $\mathbf{z} = [z_1, \cdots, z_{N_2}]^T$.

Since (29a) is an increasing function of z_i, for any given α, λ_1, and $\mathbf{p}$, the optimal $\mathbf{z}$ must satisfy the equality in (29c) which is given as

$$\sum_{i=1}^{N_2} z_i = \kappa \eta \lambda_1 + \eta \sigma_r^2 \sum_{i=1}^{N_2} (\varepsilon_i - p_i) \lambda_{2,i}. \tag{30}$$

By applying (30) to the optimization problem (29), the problem (29) is equivalently converted to

$$\max_{\alpha, \mathbf{p}, \mathbf{z}, \boldsymbol{\lambda}_2} \frac{1-\alpha}{2} \sum_{i=1}^{N_2} \log \left(1 + \frac{p_i z_i \lambda_{2,i} \lambda_{g,i}}{p_i \lambda_{2,i} + z_i \lambda_{g,i} + 1} \right) \tag{31a}$$

$$s.t.\ \sum_{i=1}^{N_2} \frac{z_i}{\sigma_r^2 \eta \lambda_{h,1}} + \sum_{i=1}^{N_2} \left(\delta_i + \frac{p_i - \varepsilon_i}{\lambda_{h,1}} \right) \lambda_{2,i} \le \frac{1+\alpha}{1-\alpha} \sigma_r^{-2} P_s \tag{31b}$$

$$\lambda_{2,i} \ge 0, \quad z_i \ge 0 \tag{31c}$$

$$0 \le p_i \le 1, \quad i = 1, \cdots, N_2 \tag{31d}$$

$$0 \le \alpha \le 1. \tag{31e}$$

Let us introduce $a_i = \delta_i^{-1}$, $b_i = \sigma_r^2 \eta \lambda_{h,1} \lambda_{g,i}$, $x_i = \delta_i \lambda_{2,i}$, $y_i = z_i / \sigma_r^2 \eta \lambda_{h,1}$, and $w_i = p_i x_i$ for $i = 1, \cdots, N_2$, the optimization

problem (31a) is rewritten into

$$\max_{\alpha,\mathbf{w},\mathbf{x},\mathbf{y}} \ \frac{1-\alpha}{2}\sum_{i=1}^{N_2}\log\left(1+\frac{a_i\,w_i\,b_i\,y_i}{1+a_iw_i+b_iy_i}\right) \tag{32a}$$

$$s.t.\ \sum_{i=1}^{N_2} y_i+\sum_{i=1}^{N_2}\frac{a_iw_i}{\lambda_{h,1}}+\sum_{i=1}^{N_2}\left(1-\frac{a_i\,\varepsilon_i}{\lambda_{h,1}}\right)x_i \le \frac{1+\alpha}{1-\alpha}\sigma_r^{-2}P_s \tag{32b}$$

$$x_i \ge w_i \ge 0, \quad y_i \ge 0,\ i=1,\cdots,N_2 \tag{32c}$$

$$0 \le \alpha \le 1 \tag{32d}$$

where $\mathbf{x}=[x_1,\cdots,x_{N_2}]^T$ and $\mathbf{y}=[y_1,\cdots,y_{N_2}]^T$. As the problem (32) is a non-convex optimization problem with multiple variables, its globally optimal solution is difficult to obtain with a tractable computational complexity. In order to solve the problem (32) with a polynomial computational complexity, in the following sections, we exploit the lower bound and the upper bound of the objective function (32a) to solve the optimization problem (32a).

IV. LOWER BOUND BASED ALGORITHM

In this section, we propose an algorithm to solve the optimization problem (32a) based on a tight lower bound of (32a) given as

$$1+\frac{a_i\,w_i\,b_i\,y_i}{1+a_i\,w_i+b_i\,y_i}=\frac{(1+a_i\,w_i)(1+b_i\,y_i)}{1+a_i\,w_i+b_i\,y_i} \ge \frac{(1+a_i\,w_i)(1+b_i\,y_i)}{2+a_i\,w_i+b_i\,y_i}. \tag{33}$$

The optimization problem (32a) is rewritten into the following

$$\min_{\alpha,\mathbf{w},\mathbf{x},\mathbf{y}} \ \frac{1-\alpha}{2}\sum_{i=1}^{N_2}\log\left(\frac{1}{1+a_i\,w_i}+\frac{1}{1+b_i\,y_i}\right) \tag{34a}$$

$$s.t.\ \sum_{i=1}^{N_2} y_i+\sum_{i=1}^{N_2}\frac{a_iw_i}{\lambda_{h,1}}+\sum_{i=1}^{N_2}\left(1-\frac{a_i\,\varepsilon_i}{\lambda_{h,1}}\right)x_i \le \frac{1+\alpha}{1-\alpha}\sigma_r^{-2}P_s \tag{34b}$$

$$x_i \ge w_i \ge 0, \quad y_i \ge 0, \quad i=1,\cdots,N_2 \tag{34c}$$

$$0 \le \alpha \le 1. \tag{34d}$$

By introducing $\widetilde{w}_i = \beta\,w_i$, $\widetilde{x}_i = \beta\,x_i$, and $\widetilde{y}_i = \beta\,y_i$ for $i=1,\cdots,N_2$, where $\beta=1-\alpha$, the optimization problem (34a) is equivalently rewritten as

$$\min_{\beta,\widetilde{\mathbf{w}},\widetilde{\mathbf{x}},\widetilde{\mathbf{y}}} \ \frac{\beta}{2}\sum_{i=1}^{N_2}\log\left(\frac{1}{1+a_i\,\widetilde{w}_i/\beta}+\frac{1}{1+b_i\,\widetilde{y}_i/\beta}\right) \tag{35a}$$

$$s.t.\ \sum_{i=1}^{N_2}\widetilde{y}_i+\sum_{i=1}^{N_2}\frac{a_i\widetilde{w}_i}{\lambda_{h,1}}+\sum_{i=1}^{N_2}\left(1-\frac{a_i\,\varepsilon_i}{\lambda_{h,1}}\right)\widetilde{x}_i \le (2-\beta)\sigma_r^{-2}P_s \tag{35b}$$

$$\widetilde{x}_i \ge \widetilde{w}_i \ge 0, \quad \widetilde{y}_i \ge 0,\ i=1,\cdots,N_2 \tag{35c}$$

$$0 \le \beta \le 1 \tag{35d}$$

where $\widetilde{\mathbf{w}}=[\widetilde{w}_1,\cdots,\widetilde{w}_{N_2}]^T$, $\widetilde{\mathbf{x}}=[\widetilde{x}_1,\cdots,\widetilde{x}_{N_2}]^T$, and $\widetilde{\mathbf{y}}=[\widetilde{y}_1,\cdots,\widetilde{y}_{N_2}]^T$. Let us introduce

$$\left(\frac{1}{\beta+a_i\,\widetilde{w}_i}+\frac{1}{\beta+b_i\,\widetilde{y}_i}\right)^{-1} \ge q_i \tag{36}$$

for $i=1,\cdots,N_2$. The optimization problem (35a) is rewritten into

$$\max_{\beta,\widetilde{\mathbf{w}},\widetilde{\mathbf{x}},\widetilde{\mathbf{y}},\mathbf{q}} \ \frac{\beta}{2}\sum_{i=1}^{N_2}\log\left(\frac{q_i}{\beta}\right) \tag{37a}$$

$$s.t.\ \left(\frac{1}{\beta+a_i\,\widetilde{w}_i}+\frac{1}{\beta+b_i\,\widetilde{y}_i}\right)^{-1} \ge q_i \quad i=1,\cdots,N_2 \tag{37b}$$

$$\sum_{i=1}^{N_2}\widetilde{y}_i+\sum_{i=1}^{N_2}\frac{a_i\widetilde{w}_i}{\lambda_{h,1}}+\sum_{i=1}^{N_2}\left(1-\frac{a_i\,\varepsilon_i}{\lambda_{h,1}}\right)\widetilde{x}_i \le (2-\beta)\sigma_r^{-2}P_s \tag{37c}$$

$$\widetilde{x}_i \ge \widetilde{w}_i \ge 0, \quad \widetilde{y}_i \ge 0,\ i=1,\cdots,N_2 \tag{37d}$$

$$0 \le \beta \le 1 \tag{37e}$$

where $\mathbf{q}=[q_1,\cdots,q_{N_2}]^T$. Since the left-hand side of (37b) is a harmonic mean, the constraint (37b) is convex [40]. Moreover, the objective function (37a) is a perspective function [40], which is concave with respect to q_i and β. Thus, the problem (37) is a convex optimization problem. By using the convex programming toolbox CVX's [41] in-built primal-dual interior-point solver, the convex problem (37) can be solved with a computational complexity of $\mathcal{O}((6N_2+2)^3)$ per iteration.

V. UPPER BOUND BASED ALGORITHM

In this section, we propose an algorithm to solve the optimization problem (32a) based on a tight upper bound of (32a) written as

$$\frac{a_i\,w_i\,b_i\,y_i}{1+a_i\,w_i+b_i\,y_i} \le \frac{a_i\,w_i\,b_i\,y_i}{a_i\,w_i+b_i\,y_i}. \tag{38}$$

By exploiting the upper bound given in (38), the optimization problem (32) is rewritten as

$$\max_{\alpha,\mathbf{w},\mathbf{x},\mathbf{y}} \ \frac{1-\alpha}{2}\sum_{i=1}^{N_2}\log\left(1+\frac{a_i\,w_i\,b_i\,y_i}{a_i\,w_i+b_i\,y_i}\right) \tag{39a}$$

$$s.t.\ \sum_{i=1}^{N_2} y_i+\sum_{i=1}^{N_2}\frac{a_iw_i}{\lambda_{h,1}}+\sum_{i=1}^{N_2}\left(1-\frac{a_i\,\varepsilon_i}{\lambda_{h,1}}\right)x_i \le \frac{1+\alpha}{1-\alpha}\sigma_r^{-2}P_s \tag{39b}$$

$$x_i \ge w_i \ge 0, \quad y_i \ge 0, \quad i=1,\cdots,N_2 \tag{39c}$$

$$0 \le \alpha \le 1. \tag{39d}$$

By applying variable substitutions of $\widetilde{w}_i$, $\widetilde{x}_i$, and $\widetilde{y}_i$ for $i=1,\cdots,N_2$, which lead to (35a), the optimization problem (39a) is equivalently converted to

$$\max_{\beta,\widetilde{\mathbf{w}},\widetilde{\mathbf{x}},\widetilde{\mathbf{y}}} \ \frac{\beta}{2}\sum_{i=1}^{N_2}\log\left(1+\frac{a_i\,(\widetilde{w}_i/\beta)\,b_i\,(\widetilde{y}_i/\beta)}{a_i\,(\widetilde{w}_i/\beta)+b_i\,(\widetilde{y}_i/\beta)}\right) \tag{40a}$$

$$s.t. \sum_{i=1}^{N_2}\widetilde{y}_i+\sum_{i=1}^{N_2}\frac{a_i\widetilde{w}_i}{\lambda_{h,1}}+\sum_{i=1}^{N_2}\left(1-\frac{a_i\,\varepsilon_i}{\lambda_{h,1}}\right)\widetilde{x}_i \le (2-\beta)\sigma_r^{-2}P_s \quad (40b)$$

$$\widetilde{x}_i \ge \widetilde{w}_i \ge 0,\ \ \widetilde{y}_i \ge 0,\ \ i=1,\cdots,N_2 \quad (40c)$$

$$0 \le \beta \le 1. \quad (40d)$$

For $i=1,\cdots,N_2$, by introducing

$$\frac{a_i\,(\widetilde{w}_i/\beta)\,b_i\,(\widetilde{y}_i/\beta)}{a_i\,(\widetilde{w}_i/\beta)+b_i\,(\widetilde{y}_i/\beta)} \ge \frac{t_i}{\beta} \quad (41)$$

the optimization problem (40a) can be rewritten as

$$\max_{\beta,\widetilde{\mathbf{w}},\widetilde{\mathbf{x}},\widetilde{\mathbf{y}},\mathbf{t}} \ \frac{\beta}{2}\sum_{i=1}^{N_2}\log\left(1+\frac{t_i}{\beta}\right) \quad (42a)$$

$$s.t. \ \frac{a_i\,(\widetilde{w}_i/\beta)\,b_i\,(\widetilde{y}_i/\beta)}{a_i\,(\widetilde{w}_i/\beta)+b_i\,(\widetilde{y}_i/\beta)} \ge \frac{t_i}{\beta} \quad (42b)$$

$$i=1,\cdots,N_2 \quad (42c)$$

$$\sum_{i=1}^{N_2}\widetilde{y}_i+\sum_{i=1}^{N_2}\frac{a_i\widetilde{w}_i}{\lambda_{h,1}}+\sum_{i=1}^{N_2}\left(1-\frac{a_i\,\varepsilon_i}{\lambda_{h,1}}\right)\widetilde{x}_i \le (2-\beta)\sigma_r^{-2}P_s \quad (42d)$$

$$\widetilde{x}_i \ge \widetilde{w}_i \ge 0,\ \ \widetilde{y}_i \ge 0,\ \ i=1,\cdots,N_2 \quad (42e)$$

$$0 \le \beta \le 1. \quad (42f)$$

From (42b), we can derive the following

$$\frac{(a_i\,(\widetilde{w}_i/\beta)+b_i\,(\widetilde{y}_i/\beta))^2-(a_i\,(\widetilde{w}_i/\beta))^2-(b_i\,(\widetilde{y}_i/\beta))^2}{2(a_i\,(\widetilde{w}_i/\beta)+b_i\,(\widetilde{y}_i/\beta))}-\frac{t_i}{\beta}\ge 0 \quad (43)$$

for $i=1,\cdots,N_2$. The inequality (43) can be equivalently expressed as

$$\begin{aligned} &a_i\,(\widetilde{w}_i/\beta)+b_i\,(\widetilde{y}_i/\beta)-2(t_i/\beta)\\ &\quad -a_i\,(\widetilde{w}_i/\beta)(a_i\,(\widetilde{w}_i/\beta)+b_i\,(\widetilde{y}_i/\beta))^{-1}a_i\,(\widetilde{w}_i/\beta)\\ &\quad -b_i\,(\widetilde{y}_i/\beta)(a_i\,(\widetilde{w}_i/\beta)+b_i\,(\widetilde{y}_i/\beta))^{-1}b_i\,(\widetilde{y}_i/\beta)\ge 0 \end{aligned} \quad (44)$$

for $i=1,\cdots,N_2$, which can be further written as a positive semidefinite (PSD) constraint given as

$$\begin{pmatrix} a_i\,\widetilde{w}_i+b_i\,\widetilde{y}_i-2t_i & a_i\,\widetilde{w}_i & b_i\,\widetilde{y}_i\\ a_i\,\widetilde{w}_i & a_i\,\widetilde{w}_i+b_i\,\widetilde{y}_i & 0\\ b_i\,\widetilde{y}_i & 0 & a_i\,\widetilde{w}_i+b_i\,\widetilde{y}_i\end{pmatrix}\ge 0. \quad (45)$$

The matrix written in (45) is a PSD matrix. By applying (45) to the optimization problem (42a), we can express the optimization problem as

$$\max_{\beta,\widetilde{\mathbf{w}},\widetilde{\mathbf{x}},\widetilde{\mathbf{y}},\mathbf{t}} \ \frac{\beta}{2}\sum_{i=1}^{N_2}\log\left(1+\frac{t_i}{\beta}\right) \quad (46a)$$

$$s.t. \begin{pmatrix} a_i\widetilde{w}_i+b_i\widetilde{y}_i-2t_i & a_i\widetilde{w}_i & b_i\widetilde{y}_i\\ a_i\widetilde{w}_i & a_i\widetilde{w}_i+b_i\widetilde{y}_i & 0\\ b_i\widetilde{y}_i & 0 & a_i\widetilde{w}_i+b_i\widetilde{y}_i\end{pmatrix} \ge 0, \quad i=1,\cdots,N_2 \quad (46b)$$

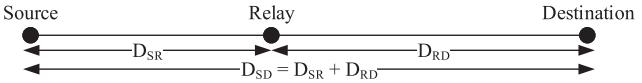

FIGURE 3. Position of source, relay, and destination nodes in the simulation.

$$\sum_{i=1}^{N_2}\widetilde{y}_i+\sum_{i=1}^{N_2}\frac{a_i\widetilde{w}_i}{\lambda_{h,1}}+\sum_{i=1}^{N_2}\left(1-\frac{a_i\,\varepsilon_i}{\lambda_{h,1}}\right)\widetilde{x}_i \le (2-\beta)\sigma_r^{-2}P_s \quad (46c)$$

$$\widetilde{x}_i \ge \widetilde{w}_i \ge 0,\quad \widetilde{y}_i \ge 0,\ i=1,\cdots,N_2 \quad (46d)$$

$$0 \le \beta \le 1. \quad (46e)$$

The optimization problem (46) is an SDP problem which can be efficiently solved by the disciplined convex programming toolbox CVX [41]. Based on [42], the computational complexity of solving the problem (46) is $\mathcal{O}(c_2(4N_2)^2(12N_2+2))$, where c_2 is the number of iterations till convergence. It will be shown in Section VI that the upper bound and lower bound based algorithms have a similar performance. This indicates that the problem (32) can be solved via the upper bound and lower bound based algorithms with a high accuracy.

VI. NUMERICAL EXAMPLES

In this section, the performance of the proposed lower bound algorithm (HPTSR-LB) and upper bound algorithm (HPTSR-UP) is investigated through numerical simulations. We consider that the source, relay, and destination nodes in the relay communication system are positioned as demonstrated in Fig. 3 for the investigation of the system performance against the relay position. The source-destination distance is set to $D_{SD}=20$ meters, where the source-relay distance is $D_{SR}=10l$ meters and the relay-destination distance is $D_{RD}=10(2-l)$ meters. The value of l $(0<l<2)$ is normalized over a distance of 10 meters. This normalization provides easy identification of the position of the relay node. For $0<l<1$, the relay position is nearer to the source node and for $1<l<2$, the relay position is nearer to the destination node. We selected $0.2\le l\le 1.8$ in the simulation such that $D_{SR}\ge 2$ m and $D_{RD}\ge 2$ m.

Similar to existing works [18], [19], [21], [22], the channel matrices are set as $\mathbf{H}=D_{SR}^{-\xi/2}\bar{\mathbf{H}}$ and $\mathbf{G}=D_{RD}^{-\xi/2}\bar{\mathbf{G}}$ where $D_{SR}^{-\xi}$ and $D_{RD}^{-\xi}$ represent the large-scale pathloss with ξ being the pathloss exponent. By considering the suburban communication scenario, we select $\xi=3$ [43]. $\bar{\mathbf{H}}$ and $\bar{\mathbf{G}}$ are constructed according to the Rayleigh fading model with their elements drawn from independent and identically distributed (i.i.d.) complex Gaussian distribution with zero mean and variances of $1/N_s$ and $1/N_r$, respectively. We consider the noise variance at the relay and destination nodes as $\sigma_r^2=\sigma_d^2=-50$dBm. The performances of both proposed algorithms are compared with the TS-based relaying (TSR) protocol for the AF MIMO relay system given in [22] and the PS-based relaying (PSR) protocol for the AF MIMO relay system given in [21]. We use the upper bound based algorithm in [22] to demonstrate the performance of the system with the TSR protocol. While the proposed method 2 in [21] which

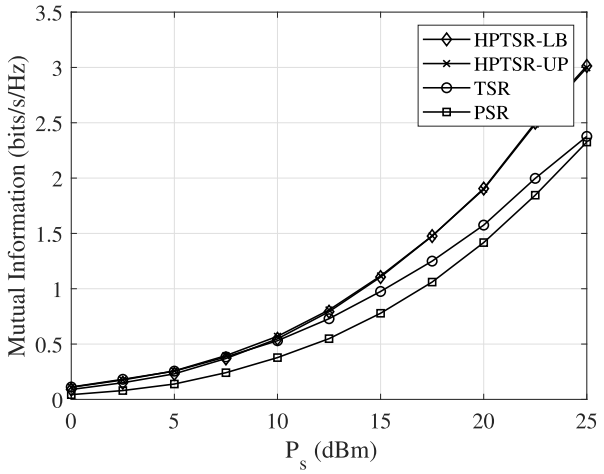

FIGURE 4. Example 1: MI versus P_S with $\eta = 0.8$, $N_S = N_r = N_d = 2$, and $l = 1$.

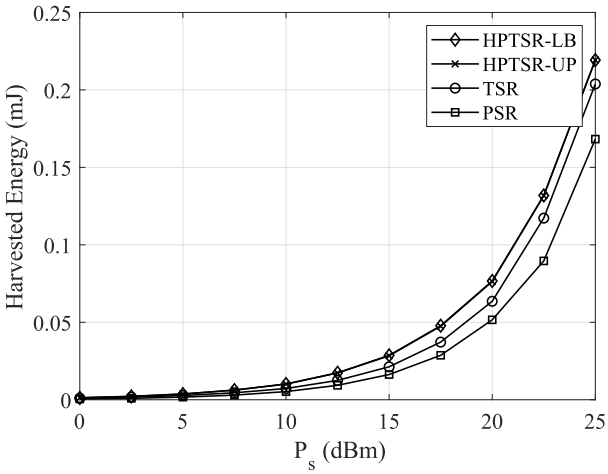

FIGURE 5. Example 1: Harvested energy at the relay node versus P_S with $\eta = 0.8$, $N_S = N_r = N_d = 2$, and $l = 1$.

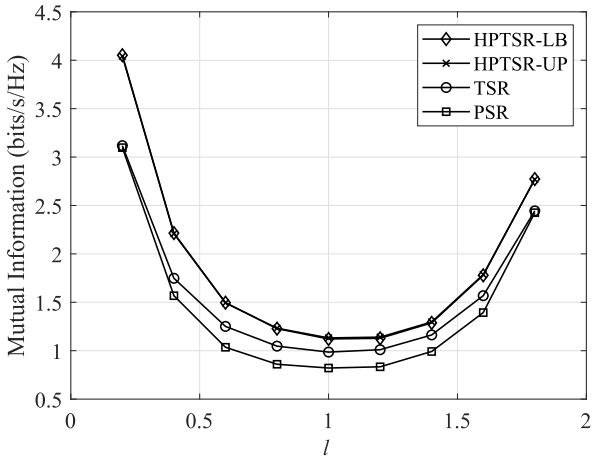

FIGURE 6. Example 2: MI versus l with $P_S = 15$dBm, $\eta = 0.8$, and $N_S = N_r = N_d = 2$.

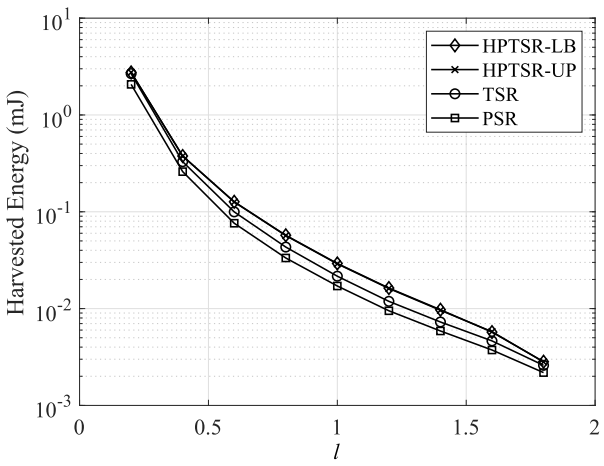

FIGURE 7. Example 2: Harvested energy at the relay node versus l with $P_S = 15$dBm, $\eta = 0.8$, and $N_S = N_r = N_d = 2$.

exploits the upper bound of the MI in the given system is used to demonstrate the performance of the system using the PSR protocol. All the numerical example results are averaged over 1000 independent channel realizations.

In the first numerical example, we set $\eta = 0.8$, $N_s = N_r = N_d = N_2 = 2$, and study the system MI of the tested algorithms versus the source node power with the relay node located at $l = 1$. Fig. 4 demonstrates the MI performance versus the source node power P_s. Fig. 5 shows the harvested energy at the relay node using the tested systems versus P_s. It is observed that the MI performance of the HPTSR-LB algorithm and the HPTSR-UP algorithm outperform the TSR algorithm given in [22] and the PSR algorithm in [21]. It is also noticed that the system performance of the HPTSR-LB algorithm is similar to that of the HPTSR-UP algorithm. With the increase of P_s, the MI gap between both the HPTSR-LB algorithm and the HPTSR-UP algorithm to the TSR algorithm as well as the PSR algorithm increases. This is because the harvested energy at the relay node using the HPTSR protocol is higher than that using the TSR protocol and the PSR protocol, which can be seen from Fig. 5. In other words, both the HPTSR-LB algorithm and the HPTSR-UP algorithm provide a higher power efficiency in terms of the MI per unit power available at the source node compared with the existing TSR algorithm and PSR algorithm, as the two proposed algorithms (HPTSR-LB and HPTSR-UP) yield a larger MI with the same transmission power budget at the source node. From the numerical results, we would like to mention that by hybridizing the TSR protocol and the PSR protocol, the system performance is greatly improved compared to the system with only the TSR protocol or the PSR protocol. This is because more degrees of freedom are provided by the HPTSR protocol for the optimization of the system performance.

In the second numerical example, we investigate the system MI of the tested algorithms at various positions of the relay node. Fig. 6 and Fig. 7 correspondingly show the MI performance and the energy harvested at the relay node of the tested algorithms versus l at $P_s = 15$dBm, $\eta = 0.8$, and $N_s = N_r = N_d = 2$. From Fig. 6 it is observed that both the HPTSR-LB algorithm and the HPTSR-UP algorithm have the highest MI at all l compared to the TSR algorithm and

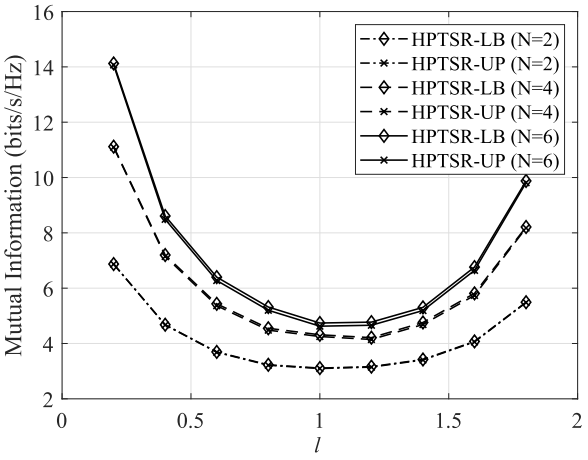

FIGURE 8. Example 3: MI versus l at various N with $P_s = 25$dBm and $\eta = 0.8$.

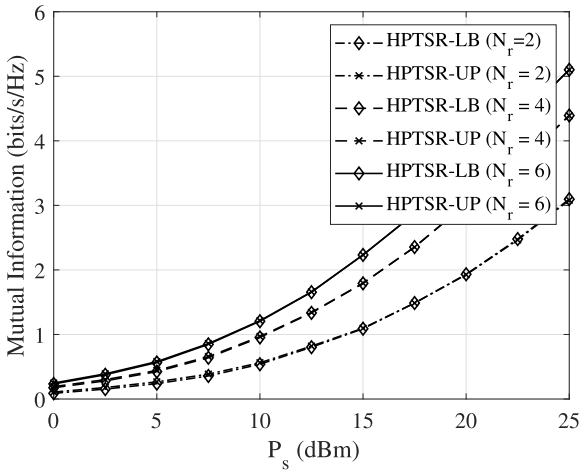

FIGURE 9. Example 3: MI versus P_S at various N_r with $l = 1$, $\eta = 0.8$, and $N_s = N_d = 2$.

the PSR algorithm. This indicates that the proposed HPTSR protocol outperforms the existing TSR protocol and PSR protocol regardless of the position of the relay node. This can be explained from Fig. 7, where it can be seen that the HPTSR-LB algorithm and the HPTSR-UP algorithm provide more harvested energy at the relay node compared to the TSR algorithm and the PSR algorithm. Besides, it is also noticeable from Fig. 7 that the harvested energy at the relay node for all the tested algorithms is reduced when the relay node is located further away from the source node. This results in the decrease of the system MI for all the tested algorithms as illustrated in Fig. 6 when $0.2 \leq l \leq 1$. However, when $1 \leq l \leq 1.8$, the system MI for all the tested algorithms as illustrated in Fig. 6 increases with l even though the available transmission energy at the relay node gained from the harvested energy reduces with l. This is due to the shorter distance between the relay and the destination nodes, which leads to a better second-hop channel and thus improves the system MI.

In the third numerical example, we investigate the MI performance of the HPTSR-LB algorithm and the HPTSR-UP algorithm at various positions of the relay node with different combinations of N_s, N_r, and N_d. Fig. 8 illustrates the system MI of the HPTSR-LB algorithm and HPTSR-UP algorithm versus l with $P_s = 25$dBm and $\eta = 0.8$ at $N_s = N_r = N_d = N$ with $N = 2$, $N = 4$, and $N = 6$. It can be noticed that the system MI increases with N. This is because with the increase of N, the number of concurrent data streams N_2 also increases which results in a higher system MI. Fig. 9 illustrates the MI performance of the proposed algorithms versus the source node power P_s with the same largest number of concurrent data streams $N_2 = N_s = N_d = 2$ when $N_r = 2$, $N_r = 4$, and $N_r = 6$ at $\eta = 0.8$ and $l = 1$. We can notice that the system with a larger number of relay antennas provides a better MI performance. This is because the relay antennas which are unused for ID are solely used for EH which also increases the energy harvested at the relay node. Thus, the MI performance of the system can be effectively improved by installing more antennas at the relay node.

VII. CONCLUSION

In this paper, we have investigated the transceiver design for a dual-hop MIMO AF relay communication system with the HPTSR-based EH relaying protocol. The architecture of the HPTSR-based protocol combines the TS-based and PS-based EH relaying protocols. The optimal structure of the source and relay precoding matrices is proposed to convert the highly challenging joint transceiver design problem to a joint transceiver power allocation problem with low complexity. Two algorithms are derived to solve the optimal power allocation problem. In general, the two proposed algorithms provide a better MI performance compared to existing TSR and PSR based algorithms. We have found that the system MI performance is better when the relay node is located closer to the source or destination nodes. Moreover, the MI performance of the system can be improved by installing more antennas at the relay node.

REFERENCES

[1] K. Xiong, P. Fan, C. Zhang, and K. B. Letaief, "Wireless information and energy transfer for two-hop non-regenerative MIMO-OFDM relay networks," *IEEE J. Sel. Areas Commun.*, vol. 33, no. 8, pp. 1595–1611, Aug. 2015.

[2] P. Kamalinejad, C. Mahapatra, Z. Sheng, S. Mirabbasi, V. C. M. Leung, and Y. L. Guan, "Wireless energy harvesting for the Internet of Things," *IEEE Commun. Mag.*, vol. 53, no. 6, pp. 102–108, Jun. 2015.

[3] J. Huang, Y. Zhou, Z. Ning, and H. Gharavi, "Wireless power transfer and energy harvesting: Current status and future prospects," *IEEE Wireless Commun.*, vol. 26, no. 4, pp. 163–169, Aug. 2019.

[4] P. Grover and A. Sahai, "Shannon meets tesla: Wireless information and power transfer," in *Proc. IEEE Int. Symp. Inf. Theory*, Austin, TX, USA, Jun. 2010, pp. 2363–2367.

[5] L. R. Varshney, "Transporting information and energy simultaneously," in *Proc. IEEE Int. Symp. Inf. Theory*, Toronto, ON, Canada, Jul. 2008, pp. 1612–1616.

[6] X. Zhou, R. Zhang, and C. K. Ho, "Wireless information and power transfer: Architecture design and rate-energy tradeoff," *IEEE Trans. Commun.*, vol. 61, no. 11, pp. 4754–4767, Nov. 2013.

[7] A. A. Nasir, X. Zhou, S. Durrani, and R. A. Kennedy, "Relaying protocols for wireless energy harvesting and information processing," *IEEE Trans. Wireless Commun.*, vol. 12, no. 7, pp. 3622–3636, Jul. 2013.

[8] Y. Rong, "MIMO relay," in *Encyclopedia of Wireless Networks*, X. Shen, X. Lin, and K. Zhang, Eds. Cham, Switzerland: Springer, 2018.

[9] Z. Ding, S. M. Perlaza, I. Esnaola, and H. V. Poor, "Power allocation strategies in energy harvesting wireless cooperative networks," *IEEE Trans. Wireless Commun.*, vol. 13, no. 2, pp. 846–860, Feb. 2014.

[10] H. Chen, Y. Li, Y. Jiang, Y. Ma, and B. Vucetic, "Distributed power splitting for SWIPT in relay interference channels using game theory," *IEEE Trans. Wireless Commun.*, vol. 14, no. 1, pp. 410–420, Jan. 2015.
[11] H. Liu, K. J. Kim, K. S. Kwak, and H. Vincent Poor, "Power splitting-based SWIPT with decode-and-forward full-duplex relaying," *IEEE Trans. Wireless Commun.*, vol. 15, no. 11, pp. 7561–7577, Nov. 2016.
[12] J. Guo, S. Zhang, N. Zhao, and X. Wang, "Performance of SWIPT for full-duplex relay system with co-channel interference," *IEEE Trans. Veh. Technol.*, vol. 69, no. 2, pp. 2311–2315, Feb. 2020.
[13] C. Zhong, H. A. Suraweera, G. Zheng, I. Krikidis, and Z. Zhang, "Wireless information and power transfer with full duplex relaying," *IEEE Trans. Commun.*, vol. 62, no. 10, pp. 3447–3461, Oct. 2014.
[14] M. Abedi, H. Masoumi, and M. J. Emadi, "Power splitting-based SWIPT systems with decoding cost," *IEEE Wireless Commun. Lett.*, vol. 8, no. 2, pp. 432–435, Apr. 2019.
[15] X. Fang, Y. Zhang, H. Cao, and N. Ying, "Spectral and energy efficiency analysis with massive MIMO systems," in *Proc. IEEE 16th Int. Conf. Commun. Technol. (ICCT)*, Hangzhou, China, Oct. 2015, pp. 837–843.
[16] Z. Ding, C. Zhong, D. Wing Kwan Ng, M. Peng, H. A. Suraweera, R. Schober, and H. V. Poor, "Application of smart antenna technologies in simultaneous wireless information and power transfer," *IEEE Commun. Mag.*, vol. 53, no. 4, pp. 86–93, Apr. 2015.
[17] B. K. Chalise, Y. D. Zhang, and M. G. Amin, "Simultaneous transfer of energy and information for MIMO-OFDM relay system," in *Proc. 1st IEEE Int. Conf. Commun. China (ICCC)*, China, Beijing, Aug. 2012, pp. 481–486.
[18] Y. Huang and B. Clerckx, "Joint wireless information and power transfer for an autonomous multiple antenna relay system," *IEEE Commun. Lett.*, vol. 19, no. 7, pp. 1113–1116, Jul. 2015.
[19] Y. Huang and B. Clerckx, "Relaying strategies for wireless-powered MIMO relay networks," *IEEE Trans. Wireless Commun.*, vol. 15, no. 9, pp. 6033–6047, Sep. 2016.
[20] J. Liao, M. R. A. Khandaker, and K.-K. Wong, "Energy harvesting enabled MIMO relaying through power splitting," in *Proc. IEEE 17th Int. Workshop Signal Process. Adv. Wireless Commun. (SPAWC)*, Edinburgh, U.K., Jul. 2016, pp. 1–5.
[21] B. Li, M. Zhang, H. Cao, Y. Rong, and Z. Han, "Transceiver design for AF MIMO relay systems with a power splitting based energy harvesting relay node," *IEEE Trans. Veh. Technol.*, vol. 69, no. 3, pp. 2376–2388, Mar. 2020.
[22] B. Li and Y. Rong, "Joint transceiver optimization for wireless information and energy transfer in nonregenerative MIMO relay systems," *IEEE Trans. Veh. Technol.*, vol. 67, no. 9, pp. 8348–8362, Sep. 2018.
[23] B. Li, H. Cao, Y. Rong, T. Su, G. Yang, and Z. He, "Transceiver optimization for DF MIMO relay systems with a wireless powered relay node," *IEEE Access*, vol. 7, pp. 56904–56919, Apr. 2019.
[24] F. Benkhelifa and M.-S. Alouini, "Precoding design of MIMO amplify-and-forward communication system with an energy harvesting relay and possibly imperfect CSI," *IEEE Access*, vol. 5, pp. 578–594, 2017.
[25] F. Benkhelifa, A. S. Salem, and M.-S. Alouini, "Rate maximization in MIMO decode-and-forward communications with an EH relay and possibly imperfect CSI," *IEEE Trans. Commun.*, vol. 64, no. 11, pp. 4534–4549, Nov. 2016.
[26] F. K. Ojo and M. F. Mohd Salleh, "Secrecy analysis of SWIPT-enabled cooperative networks with DF HPTSR protocol," *IEEE Access*, vol. 6, pp. 65996–66006, 2018.
[27] Y. Liu, R. Xiao, J. Shen, H. Yang, and C. Yan, "Performance analysis for hybrid AF relaying protocol in SWIPT systems with direct link," in *Proc. IEEE/CIC Int. Conf. Commun. Workshops China (ICCC Workshops)*, Changchun, China, Aug. 2019, pp. 109–113.
[28] F. K. Ojo and M. F. Mohd Salleh, "Throughput analysis of a hybridized power-time splitting based relaying protocol for wireless information and power transfer in cooperative networks," *IEEE Access*, vol. 6, pp. 24137–24147, 2018.
[29] R. Xiao, Y. Liu, H. Yang, J. Shen, and C. Yan, "Performance analysis of hybrid protocol based two-way Decode-and-Forward relay networks," in *Proc. IEEE 4th Int. Conf. Comput. Commun. (ICCC)*, Chengdu, China, Dec. 2018, pp. 146–151.
[30] R. Zhang and C. K. Ho, "MIMO broadcasting for simultaneous wireless information and power transfer," *IEEE Trans. Wireless Commun.*, vol. 12, no. 5, pp. 1989–2001, May 2013.
[31] Z. Popovic, E. A. Falkenstein, D. Costinett, and R. Zane, "Low-power far-field wireless powering for wireless sensors," *Proc. IEEE*, vol. 101, no. 6, pp. 1397–1409, Jun. 2013.
[32] H. J. Visser and R. J. M. Vullers, "RF energy harvesting and transport for wireless sensor network applications: Principles and requirements," *Proc. IEEE*, vol. 101, no. 6, pp. 1410–1423, Jun. 2013.
[33] S. D. Assimonis, S.-N. Daskalakis, and A. Bletsas, "Sensitive and efficient RF harvesting supply for batteryless backscatter sensor networks," *IEEE Trans. Microw. Theory Techn.*, vol. 64, no. 4, pp. 1327–1338, Apr. 2016.
[34] C. R. Valenta and G. D. Durgin, "Harvesting wireless power: Survey of energy-harvester conversion efficiency in far-field, wireless power transfer systems," *IEEE Microw. Mag.*, vol. 15, no. 4, pp. 108–120, Jun. 2014.
[35] D. Darsena, "Noncoherent detection for ambient backscatter communications over OFDM signals," *IEEE Access*, vol. 7, pp. 159415–159425, 2019.
[36] A. W. Marshall and I. Olkin, *Inequalities: Theory of Majorization and Its Applications*. New York, NY, USA: Academic, 1980.
[37] A. Chervov, G. Falqui, and V. Rubtsov, "Algebraic properties of manin matrices 1," *Adv. Appl. Math.*, vol. 43, no. 3, pp. 239–315, Sep. 2009.
[38] J. Hadamard, "Resolution d'une question relative aux determinants," *Bull. des Sci. Math.*, vol. 2, no. 17, pp. 240–246, Sep. 1893.
[39] Y. Rong, X. Tang, and Y. Hua, "A unified framework for optimizing linear nonregenerative multicarrier MIMO relay communication systems," *IEEE Trans. Signal Process.*, vol. 57, no. 12, pp. 4837–4851, Dec. 2009.
[40] S. Boyd and L. Vandenberghe, *Convex Optimization*. Cambridge, U.K.: Cambridge Univ. Press, 2004.
[41] M. Grant and S. Boyd. (Apr. 2010). *CVX: MATLAB Software for Disciplined Convex Programming*. [Online]. Available: http://cvxr.com/cvx
[42] Y. Nesterov and A. Nemirovskii, *Interior-Point Polynomial Algorithms in Convex Programming*. Philadelphia, PA, USA: Society for industrial and applied mathematics, 1994.
[43] C. Song, J. Park, B. Clerckx, I. Lee, and K.-J. Lee, "Generalized precoder designs based on weighted MMSE criterion for energy harvesting constrained MIMO and multi-user MIMO channels," *IEEE Trans. Wireless Commun.*, vol. 15, no. 12, pp. 7941–7954, Dec. 2016.

JUSTIN LEE BING (Student Member, IEEE) received the B.E. (Hons.) degree in electronic and communication engineering from Curtin University, Australia, in 2016. He is currently pursuing the Ph.D. degree with the Department of Electrical and Computer Engineering, Curtin University Malaysia. His research interests include wireless communications, signal processing for communications, simultaneous wireless information, power transfer, and energy harvesting.

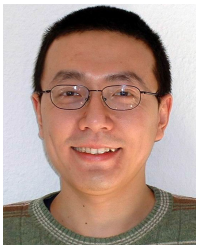

YUE RONG (Senior Member, IEEE) received the Ph.D. degree *(summa cum laude)* in electrical engineering from the Darmstadt University of Technology, Darmstadt, Germany, in 2005.

He was a Postdoctoral Researcher with the Department of Electrical Engineering, University of California, Riverside, from February 2006 to November 2007. Since December 2007, he has been with Curtin University, Bentley, WA, Australia, where he is currently a Professor. He has published over 170 journal and conference papers in these areas. His research interests include signal processing for communications, wireless communications, underwater acoustic communications, underwater optical wireless communications, applications of linear algebra and optimization methods, and statistical and array signal processing. He was a TPC Member of the IEEE ICC, the IEEE GlobalSIP, EUSIPCO, the IEEE ICCC, WCSP, IWCMC, and ChinaCom. He was a recipient of the Best Paper Award from the 2011 International Conference on Wireless Communications and Signal Processing, the Best Paper Award from the 2010 Asia-Pacific Conference on Communications, and the Young Researcher of the Year Award from the Faculty of Science and Engineering, Curtin University, in 2010. He served as an Editor for the IEEE Wireless Communications Letters from 2012 to 2014, an Associate Editor for the IEEE Transactions on Signal Processing from 2014 to 2018, and a Guest Editor for the IEEE Journal on Selected Areas in Communications Special Issue on Theories and Methods for Advanced Wireless Relays. He serves as a Senior Area Editor for the IEEE Transactions on Signal Processing.

LENIN GOPAL (Member, IEEE) received the B.Eng. degree in electrical and electronics engineering from Madurai Kamaraj University, Madurai, India, in 1996, the M.Eng. degree in telecommunications engineering from Multimedia University, Cyberjaya, Malaysia, in 2006, and the Ph.D. degree from Curtin University, Bentley, WA, Australia, in 2015. He is currently an Associate Professor with the Department of Electrical and Computer Engineering, Faculty of Engineering and Science, Curtin University Malaysia, Miri, Malaysia. His research interests include signal processing for communications, power line communications, and the Internet of Things (IoTs).

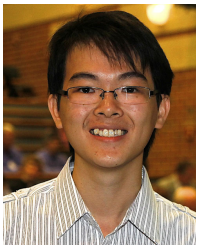

CHOO W. R. CHIONG (Member, IEEE) received the B.E. (Hons.) and Ph.D. degrees in electrical engineering from Curtin University, Bentley, WA, Australia, in 2010 and 2015, respectively. He is currently a Senior Lecturer with the Department of Electrical and Computer Engineering, Curtin University Malaysia. His research interests include signal processing for communications and power system optimization.